Prospects on the search for invisible Higgs decays in the ZH channel at the LHC and HL-LHC: A Snowmass White Paper

Hideki Okawa¹, Josh Kunkle², and Elliot Lipeles²

¹Brookhaven National Laboratory, Upton, NY, USA ²University of Pennsylvania, Philadelphia, PA, USA

Abstract

We show prospects on a search for invisible decays of a Higgs boson at the Large Hadron Collider (LHC) and High Luminosity LHC (HL-LHC). This search is performed on a Higgs boson produced in association with a Z boson. We expect that the branching ratio of 17-22% (6-14%) could be excluded at 95% confidence level with 300 fb⁻¹ (3000 fb⁻¹) of data at $\sqrt{s} = 14$ TeV. The range indicates different assumptions on the control of systematic uncertainties. Interpretations with Higgs-portal dark matter models are also considered.

1 Introduction

The nature of dark matter is an outstanding question in particle physics and cosmology. One possible explanation is a weakly interacting massive particle (WIMP) that is thermally produced in the early universe. If such a WIMP exists and has a mass less than half the Higgs mass, the Higgs could decay into WIMP pairs, which would result in the Higgs boson having an invisible branching ratio larger than the Standard Model expectation. Limits on the Higgs to invisible branching ratio from the Large Hadron Collider (LHC) place constraints on the Higgs to WIMP couplings comparable to direct detection experiments. For low WIMP masses ($\lesssim 10 \text{ GeV}$), direct detection limits are significantly weaker because recoil energy of a struck nucleon is lower and the corresponding signal is more difficult to differentiate from backgrounds. This is the region where Higgs decay is particularly sensitive leading to a strong complementarity with direct detection experiments (described in Section 4.3).

We describe here the estimated future sensitivity of searches for Higgs decaying invisibly using the ZH channel [1,2]. Both ATLAS and CMS have reported preliminary limits on the invisible branching ratio of the Higgs using the ZH channel with Z decaying to electrons or muons and the invisible Higgs identified by a missing energy signature [3,4]. The 95% confidence level (CL) limits for ATLAS and CMS are 65% observed, 84% expected and 75% observed, 91% expected, respectively. The vector boson fusion channel is known to have comparable sensitivity [5–7], and CMS recently

reported 95% CL limits of 69% observed and 53% expected on the invisible branching fraction [8]. As a complementary approach, combined coupling measurements of the Higgs boson allow for setting an indirect bound on the invisible and undetectable modes, which is 60% at 95% CL for ATLAS [9].

For the ZH channel, the significant backgrounds for this search in order of importance are: $ZZ \to \ell^+\ell^-\nu\bar{\nu}$, $WZ \to \ell\nu\ell^+\ell^-$ where one lepton is not identified, $W^+W^- \to \ell^+\nu\ell^-\bar{\nu}$, $t\bar{t} \to b\bar{b}\ell^+\nu\ell^-\bar{\nu}$ and $Wt \to \ell\nu\ell\nu$ which are suppressed by a jet veto, $Z \to \ell^+\ell^-$ with false missing energy, and W^+ jets, $t\bar{t} \to b\bar{b}\ell\nu qq$ and s/t-channel single top quark with a jet misidentified as a lepton. There are two main issues in scaling this result to higher luminosities: the effect of pile-up on the Z background and the systematic uncertainty on the ZZ background. It should be noted that requirement for the angular difference between a track-based missing transverse momentum ($\vec{p}_{\rm T}^{\rm miss}$) and object-based missing transverse energy ($\vec{E}_{\rm T}^{\rm miss}$; $E_{\rm T}^{\rm miss}$ for the magnitude) is not used in the Delphes study, which could lead to a weaker estimated limit than what might actually be attainable. On the other hand, optimistic assumptions on pileup effects, if any, especially on the $E_{\rm T}^{\rm miss}$ and jets could lead to a stronger estimated limit.

2 Signal and Background Samples

The signal and background simulation samples are generated with MADGRAPH5 [10] with PYTHIA6 [11] parton showering and hadronization. All of these samples are processed through the Delphes fast detector simulation [12–14].

We used the official Snowmass background samples, and privately produced signal samples following the official Snowmass configurations for the pileup scenarios: $\langle \mu \rangle = 50~(\mu)$: mean number of interactions per crossing) for the LHC Phase-I with expected integrated luminosity of 300 fb⁻¹ and $\langle \mu \rangle = 140$ for the LHC Phase-II also known as the High Luminosity LHC (HL-LHC) with 3000 fb⁻¹. All the processes are normalized to the next-to-leading order (NLO) cross sections. For the invisible Higgs boson signal, the mass of 125 GeV and the Standard Model cross section value of the ZH production are assumed.

3 Object and Event Selection

We use the reconstructed objects from the Delphes detector simulation, which include contributions from the pileup. Events are selected to have two charged leptons (electrons or muons) and large $E_{\rm T}^{\rm miss}$. While the $E_{\rm T}^{\rm miss}$ requirement suppresses the Drell-Yan background, an additional jet-veto is used to suppress the top backgrounds.

As we consider events with a Z boson and large $E_{\rm T}^{\rm miss}$, we require two oppositely-charged electrons or muons with an invariant mass between 76 to 106 GeV. Electrons (muons) are required to have $p_T > 20$ GeV and $|\eta| < 2.47$ (2.5). In order to reduce the $WZ \to \ell\nu\ell^+\ell^-$ background, events with additional lower threshold electrons and muons ($p_T > 7$ GeV) are vetoed. Figure 1 shows the $E_{\rm T}^{\rm miss}$ distributions for the events after requiring a dilepton in the Z mass window.

Our analysis is based on the ATLAS event selection [3] with the following modifications.

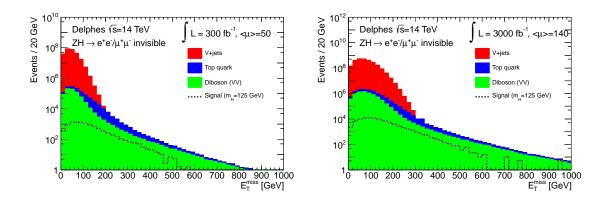


Figure 1: $E_{\rm T}^{\rm miss}$ distributions after the dilepton mass requirement for the 14 TeV LHC and HL-LHC scenarios. The stacked histograms represent the background predictions from the Delphes samples. The Delphes samples are inclusively generated for various bosons, and "V" stands for W, Z, γ , and H. The signal hypothesis is shown by a dotted line and assumes the SM ZH production rate for a $m_H = 125$ GeV Higgs boson with a 100% invisible branching ratio.

Cut variables	Thresholds (LHC, $\langle \mu \rangle = 50$)	Thresholds (HL-LHC, $\langle \mu \rangle = 140$)
$E_{\mathrm{T}}^{\mathrm{miss}}$	> 150 GeV	> 170 GeV
$\mathrm{d}\phi(\ell,\ell)$	< 1.4	< 1.1
$\mathrm{d}\phi(\vec{p}_T^{\ell,\ell},\vec{E}_\mathrm{T}^\mathrm{miss})$	> 2.6	> 2.6
$ E_{\mathrm{T}}^{\mathrm{miss}}-p_{T}^{\ell,\ell} /p_{T}^{\ell,\ell}$	< 0.3	< 0.4
Jet veto	> 45 GeV	> 60 GeV

Table 1: Event selection optimized for the LHC and HL-LHC scenarios at 14 TeV.

- The $E_{\rm T}^{\rm miss}$ is required to be larger than 150 GeV for 300 fb⁻¹ and 170 GeV for 3000 fb⁻¹.
- The $\vec{p}_{T}^{\text{miss}}$ is not considered.
- The p_T threshold for the jet veto is raised to 45 GeV for 300 fb⁻¹ and 60 GeV for 3000 fb⁻¹, as the jet reconstruction in the Delphes simulation does not correct for the pileup.
- Some of the angular cuts with the $\vec{E}_{\mathrm{T}}^{\mathrm{miss}}$ are relaxed, because the correlation of the $\vec{E}_{\mathrm{T}}^{\mathrm{miss}}$ with the dilepton system is degraded due to the pileup.

The thresholds are chosen to increase the signal sensitivity. The event selection used in this analysis is summarized in Table 1. Figure 2 shows the distributions of the kinematic variables used in the event selection for the events after requiring a dilepton in the Z mass window.

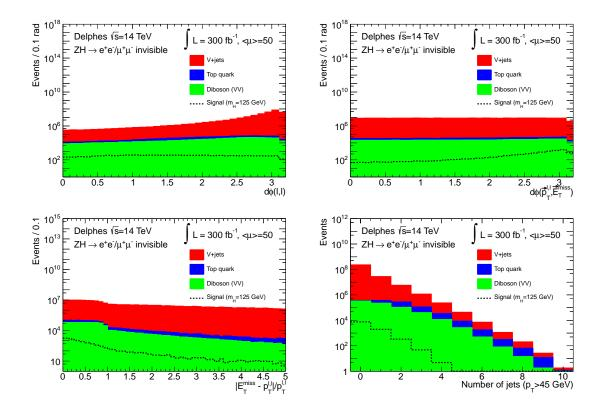


Figure 2: Distributions of kinematic variables after the dilepton mass requirement for the LHC scenario. The stacked histograms represent the background predictions from the Delphes samples. The Delphes samples are inclusively generated for various bosons, and "V" stands for W, Z, γ , and H. The signal hypothesis is shown by a dotted line and assumes the SM ZH production rate for a $m_H = 125$ GeV Higgs boson with a 100% invisible branching ratio.

4 Results

Table 2 shows the expected background and signal yields for the two luminosity scenarios. Only the statistical uncertainty from the Delphes samples is shown in the table. The Z and W backgrounds do not remain after applying the event selection for the LHC scenario. Very few top events remain after the jet veto cut, and thus lead to a large statistical uncertainty.

4.1 Systematics

We consider two scenarios for the size of systematics.

For the conservative scenario, experimental uncertainty of 5%, theoretical uncertainty of 5%, and jet veto systematics of 6% are assumed for the diboson backgrounds.

For the realistic case, the uncertainty is expected to become smaller using data-driven methods, making use of the large data statistics. From the expected yields of the $ZZ \to 4\ell$, the ZZ background would be estimated within 6% for 300 fb⁻¹ and 2% for 3000 fb⁻¹. We adopt this uncertainty for the diboson backgrounds.

For both scenarios, the top quark background is estimated to have the overall

Expected yields	LHC (300 fb^{-1})	$HL-LHC (3000 \text{ fb}^{-1})$
Dibosons $(ZZ, WZ, WW, \text{ etc.})$	1754 ± 29	12009 ± 203
$t\bar{t}$, single top	2.4 ± 1.4	550 ± 530
Single boson $(Z/W + jets, etc.)$	_	1199 ± 599
Signal (125 GeV, BR($H \rightarrow \text{inv.}$)=20%)	217 ± 5	1517 ± 40

Table 2: Expected background and signal yields for the LHC and HL-LHC scenarios. The statistical uncertainty from the Delphes samples is shown.

BR($H \rightarrow \text{inv.}$) limits at 95% (90%) CL	LHC (300 fb^{-1})	$HL-LHC (3000 \text{ fb}^{-1})$
No systematics	7.5% (6.2%)	$2.9\% \ (2.5\%)$
Realistic scenario	17% (14%)	6.2% (5.2%)
Conservative scenario	22% (19%)	14% (11%)

Table 3: Expected limits with 95% (90%) CL on the invisible branching ratio of the Higgs boson are shown for the LHC and HL-LHC scenarios. The Standard Model cross section for the ZH production is assumed.

uncertainty of 9% for 300 fb⁻¹ and 3% for 3000 fb⁻¹, extrapolating the expected yields in the $e\mu$ control region from Ref. [3].

The Z background is assumed to have the uncertainty of 10%, but this background is expected to be suppressed significantly by the $d\phi(\vec{E}_{\rm T}^{\rm miss}, \vec{p}_{\rm T}^{\rm miss})$ selection, which is not applied in this paper.

For the signals, the experimental uncertainty of 5%, theoretical uncertainty of 5%, and jet veto systematics of 6% are considered for all cases.

During the limit setting, the correlation between the signals and the diboson backgrounds is taken into account for the jet veto systematics.

4.2 Sensitivity

We calculated the limits with the CL_s modified frequentist formalism [15] using a maximum likelihood fit using the $E_{\rm T}^{\rm miss}$ distributions with a profile likelihood test statistics [16].

Table 3 shows the expected limits with various size of systematic uncertainty on the background and signal. For the HL-LHC scenario, the Z background is concentrated at the lowest $E_{\rm T}^{\rm miss}$ bin, thus the signal sensitivity still remains to be high. The 90% CL limits are also shown to be compared with direct detection dark matter experiments in Section 4.3. The dominant systematics is the ZZ normalization. The current LHC results [3, 4] quote uncertainties between 7% and 11%. The Higgs to WW measurements are able to use control regions to normalize similar backgrounds to better than 2% [17].

4.3 Interpretation with Higgs-Portal Models

A possible interpretation of the invisible decay of the Higgs boson is in the context of dark matter particles coupling to the Higgs boson. Such dark matter models are called the Higgs-portal models [18–21].

The model considered here introduces dark matter as a single new particle that couples only with the Higgs boson. The strength of the interaction between the dark matter and the Higgs boson is given by the coupling constant, $\lambda_{h\chi\chi}$. Within the Higgs-portal models, limits from the invisible branching ratio of the Higgs can be compared to limits from dark matter direct detection experiments. This is possible because the scattering process to which direct detection experiments are sensitive is related to the decay process used here by the coupling constant. The relationship between the decay width, the coupling constant, and the dark matter-nucleon scattering cross section depend on the spin of the dark matter particle [19–22]. We consider three spin scenarios: a scalar, vector, or majorana-fermion.

Figure 3 shows the upper limits on the dark matter-nucleon scattering cross section. The expected limits from the "realistic scenario" in Table 3 are used for the interpretation. In expressing the invisible branching fraction limits in terms of the dark matter-nucleon scattering cross section, the nucleon form factor, f_N , must be included to parametrize the coupling between the Higgs boson and the nucleon. The nucleon form factor is taken as $0.326^{+0.303}_{-0.066}$ [20]. Its uncertainty is expressed as systematics bands in the figure. To be consistent with the direct detection experiments [23–30], we use 90% CL limits to map the branching ratio bounds. Figure 4 shows the upper limits on the Higgs-dark matter couplings.

In the context of the Higgs-portal models, the LHC has an outstanding sensitivity for the mass region of the dark matter below half the Higgs mass.

5 Conclusions

We showed prospects on a direct search for invisible decays of a Higgs boson at the LHC and HL-LHC. This search is performed on a Higgs boson produced in association with a Z boson. We expect that the branching ratio of 17-22% (6-14%) could be excluded at 95% confidence level with 300 fb⁻¹ (3000 fb⁻¹) of data at $\sqrt{s} = 14$ TeV. The range indicates different assumptions on the control of systematic uncertainties. We interpret the results in the context of Higgs-portal models, which shows a strong complementarity between invisible Higgs decay searches and direct dark matter searches.

Acknowledgments

JK acknowledges Yann Mambrini, Joachim Kopp, and Gary Steigman for useful discussions regarding the dark matter interpretations. HO thanks Hong Ma and Marc-Andre Pleier for fruitful conversations. This work was supported by the US Department of Energy under Contract No. DE-AC02-98CH10886 and DE-SC0007901.

References

[1] R. Godbole, M. Guchait, K. Mazumdar, S. Moretti, and D. Roy, Search for 'invisible' Higgs signals at LHC via associated production with gauge bosons,

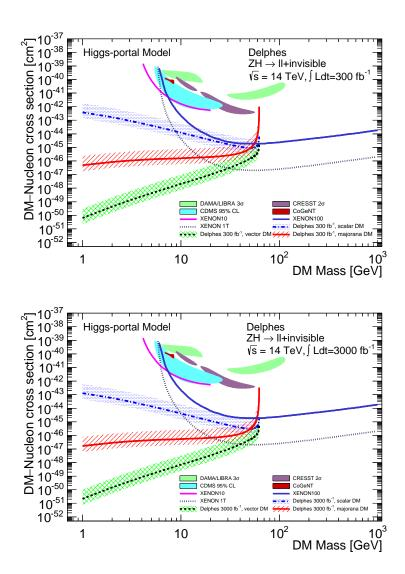


Figure 3: 90% C.L. upper limits on the dark matter-nucleon scattering cross section in Higgs-portal scenarios, extracted from the expected Higgs to invisible branching fraction limit and from direct-search experiments. The results are shown for three model variants in which the DM candidate is a scalar, vector or fermion particle. The hashed areas correspond to the uncertainty of the nucleon form factor.

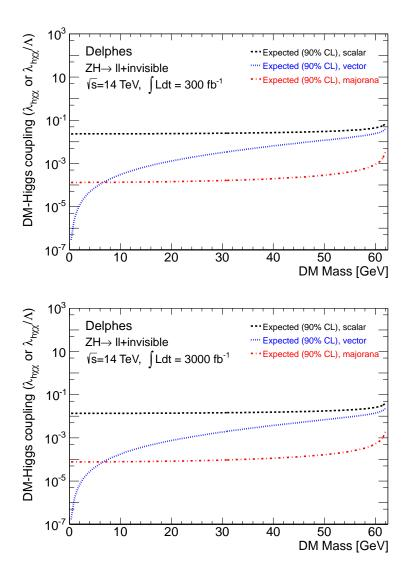


Figure 4: 90% CL limits on the Higgs-dark matter couplings in Higgs-portal scenarios, extracted from the expected Higgs to invisible branching fraction limit. The results are shown for three model variants in which the dark matter candidate is a scalar, vector or fermion particle.

- Phys.Lett. **B571** (2003) 184-192, arXiv:hep-ph/0304137 [hep-ph].
- [2] D. Ghosh, R. Godbole, M. Guchait, K. Mohan, and D. Sengupta, Looking for an Invisible Higgs Signal at the LHC, Phys.Lett. B725 (2013) 344–351, arXiv:1211.7015 [hep-ph].
- [3] ATLAS Collaboration, Search for invisible decays of a Higgs boson produced in association with a Z boson in ATLAS, ATLAS-CONF-2013-011 (2013).
- [4] CMS Collaboration, Search for invisible decays of a Higgs boson produced in association with a Z boson, CMS-PAS-HIG-13-018 (2013).
- [5] O.J.P. Eboli, D. Zeppenfeld, *Observing an invisibly Higgs boson*, Phys. Lett. **B495** (2000) 147, arXiv:hep-ph/0009158.
- [6] B. Di Girolamo, L. Neukermans, K. Mazumdar, A. Nikitenko, D. Zeppenfeld, Experimental Observation of an invisible Higgs Boson at LHC: The Higgs Working Group Summary Report, Workshop on Physics at TeV Colliders, Les Houches, France, 2001 (2001), arXiv:hep-ph/0203056.
- [7] ATLAS Collaboration, Sensitivity to an Invisibly Decaying Higgs Boson; Expected performance of the ATLAS experiment: detector, trigger and physics, CERN-OPEN-2008-020 (2008).
- [8] CMS Collaboration, Search for invisible Higgs decays in the VBF channel, CMS-PAS-HIG-13-013 (2013).
- [9] ATLAS Collaboration, Combined coupling measurements of the Higgs-like boson with the ATLAS detector using up to 25 fb⁻¹ of proton-proton collision data, ATLAS-CONF-2013-034 (2013).
- [10] J. Alwall, M. Herquet, F. Maltoni, O. Mattelaer, and T. Stelzer, *MadGraph 5:* Going Beyond, JHEP **1106** (2011) 128, arXiv:1106.0522.
- [11] T. Sjostrand, S. Mrenna and P. Z. Skands, *PYTHIA 6.4 Physics and Manual*, JHEP **0605** (2006) 026, arXiv:hep-ph/0603175.
- [12] J. Anderson et al., Snowmass Energy Frontier Simulations, arXiv:1309.1057.
- [13] A. Avetisyan et al., Methods and Results for Standard Model Event Generation at $\sqrt{s} = 14$ TeV, 33 TeV, and 100 TeV Proton Colliders, arXiv:1308.1636.
- [14] A. Avetisyan et al., Snowmass Energy Frontier Simulations using the Open Science Grid, arXiv:1308.0843.
- [15] A.L. Read, Presentation of search results: The CLs technique, J. Phys. G 28 (2002) 2693–2704.
- [16] G. Cowan, K. Cranmer, E. Gross, O. Vitells, Asymptotic formulae for likelihood-based tests of new physics, Eur. Phys. J. C 71 (2011) 1554.

- [17] ATLAS Collaboration, Measurements of the properties of the Higgs-like boson in the $WW^{(*)} \rightarrow \ell\nu\ell\nu$ decay channel with the ATLAS detector using 25 fb⁻¹ of proton-proton collision data, ATLAS-CONF-2013-030 (2013).
- [18] B. Patt and F. Wilczek, *Higgs-field portal into hidden sectors*, arXiv:hep-ph/0605188.
- [19] P. J. Fox, R. Harnik, J. Kopp, and Y. Tsai, Missing Energy Signatures of Dark Matter at the LHC, Phys.Rev. D85 (2012) 056011, arXiv:1109.4398 [hep-ph].
- [20] A. Djouadi, O. Lebedev, Y. Mambrini, and J. Quevillon, *Implications of LHC searches for Higgs-portal dark matter*, Phys.Lett. B709 (2012) 65–69, arXiv:1112.3299 [hep-ph].
- [21] L. Lopez-Honorez, T. Schwetz, and J. Zupan, Higgs portal, fermionic dark matter, and a Standard Model like Higgs at 125 GeV, Phys.Lett. B716 (2012) 179–185, arXiv:1203.2064 [hep-ph].
- [22] S. Kanemura, S. Matsumoto, T. Nabeshima, and N. Okada, Can WIMP dark matter overcome the nightmare scenario?, Phys. Rev. **D82** (2010) 055026.
- [23] J. Angle et al. (XENON10 Collaboration), Search for Light Dark Matter in XENON10 Data, Phys. Rev. Lett. 107 (2011) 051301.
- [24] E. Aprile et al. (XENON100 Collaboration), Dark Matter Results from 225 Live Days of XENON100 Data, Phys. Rev. Lett. 109 (2012) 181301.
- [25] K. Arisaka for XENON Collaboration, The XENON Dark Matter Program at LNGS: XENON100, 1T and beyond, Snowmass Cosmic Frontier Workshop, March 6-8, 2013.
- [26] G. Angloher et al., Results from 730 kg days of the CRESST-II Dark Matter Search, Eur. Phys. J. C 72 (2012) 1971.
- [27] R. Bernabei et al., First results from DAMA/LIBRA and the combined results with DAMA/NaI, Eur. Phys. J. C56 (2008) 333.
- [28] CoGeNT Collaboration, Search for an Annual Modulation in a P-type Point Contact Germanium Dark Matter Detector, Phys.Rev.Lett. 107 (2011) 141301, arXiv:1106.0650 [astro-ph].
- [29] P. Fox, J. Kopp, M. Lisanti, and N. Weiner, A CoGeNT Modulation Analysis, Phys. Rev. D 85 (2012) 036008.
- [30] R. Agnese et al. (CDMS Collaboration), Dark Matter Search Results Using the Silicon Detectors of CDMS II, Phys. Rev. Lett. 111 (2013) 251301.